3. A. Bring *et al.*, Implications of freshwater flux data from the CMIP5 multimodel output across a set of Northern Hemisphere drainage basins. *Earths Future* 2014EF000296 (2015).
4. P. C. D. Milly *et al.*, *Science* **319**, 573–574 (2008).
5. F. Jaramillo, G. Destouni, *Geophys. Res. Lett.* **41**, 8377–8386 (2014).
6. G. Destouni, F. Jaramillo, C. Prieto, *Nat. Clim. Change* **3**, 213–217 (2013).
7. C. Nilsson, C. A. Reidy, M. Dynesius, C. Revenga, *Science* **308**, 405–408 (2005).
8. World Commission on Dams, *Dams and Development: A New Framework for Decision-Making* (Dams and Development Project, United Nations Environment Programme, Nairobi Kenya; Earthscan, London, 2000).
9. B. Lehner *et al.*, *Front. Ecol. Environ* **9**, 494–502 (2011).
10. S. Siebert, V. Henrich, K. Frenken, J. Burke, *Global Map of Irrigation Areas*, version 5 (Rheinische Friedrich-Wilhelms-University, Bonn, Germany/Food and Agriculture Organization of the United Nations, Rome, Italy, 2013).
11. M. Dynesius, C. Nilsson, *Science* **266**, 753–762 (1994).
12. C. J. Vörösmarty *et al.*, *Ambio* **26**, 210–219 (1997).
13. Y. Shibuo, J. Jarsjö, G. Destouni, *Geophys. Res. Lett.* **34**, L21406 (2007).
14. L. Levi, F. Jaramillo, R. Andričević, G. Destouni, *Ambio* **44**, 624–634 (2015).
15. N. L. Poff, J. D. Olden, D. M. Merritt, D. M. Pepin, *Proc. Natl. Acad. Sci. U.S.A.* **104**, 5732–5737 (2007).
16. P. Döll, K. Fiedler, J. Zhang, *Hydrol. Earth Syst. Sci.* **13**, 2413–2432 (2009).
17. O. Boucher, G. Myhre, A. Myhre, *Clim. Dyn.* **22**, 597–603 (2004).
18. S. Piao *et al.*, *Proc. Natl. Acad. Sci. U.S.A.* **104**, 15242–15247 (2007).
19. S. Rost, D. Gerten, U. Heyder, *Adv. Geosci.* **18**, 43–50 (2008).
20. I. Haddeland, T. Skaugen, D. P. Lettenmaier, *Geophys. Res. Lett.* **33**, L08406 (2006).
21. S. M. Sterling, A. Ducharne, J. Polcher, *Nat. Clim. Change* **3**, 385–390 (2013).
22. M. I. Budyko, *Climate and Life* (Academic Press, 1974).
23. V. K. Arora, *J. Hydrol. (Amst.)* **265**, 164–177 (2002).
24. P. C. D. Milly, *Water Resour. Res.* **30**, 2143–2156 (1994).
25. W. R. Berghuijs, R. A. Woods, M. Hrachowitz, *Nat. Clim. Change* **4**, 583–586 (2014).
26. S. Siebert *et al.*, *Hydrol. Earth Syst. Sci.* **14**, 1863–1880 (2010).
27. W. Steffen *et al.*, *Science* **347**, 1259855 (2015).
28. A. Y. Hoekstra, M. M. Mekonnen, *Proc. Natl. Acad. Sci. U.S.A.* **109**, 3232–3237 (2012).
29. M. M. Mekonnen, A. Y. Hoekstra, *Hydrol. Earth Syst. Sci.* **15**, 1577–1600 (2011).
30. A. Y. Hoekstra, T. O. Wiedmann, *Science* **344**, 1114–1117 (2014).
31. S. Rost *et al.*, *Water Resour. Res.* **44**, W09405 (2008).
32. M. M. Mekonnen, A. Y. Hoekstra, *Hydrol. Earth Syst. Sci.* **16**, 179–187 (2012).

ACKNOWLEDGMENTS

The Swedish Research Council (VR, project 2009-3221), the strategic environmental research project Ekoklim at Stockholm University, and the BECC strategic research area of Lund University and the University of Gothenburg have funded this study. All data used in our analysis are included in the supplementary materials available on *Science* Online. The authors thank the anonymous reviewers for their suggestions and recommendations, which have considerably improved this manuscript, as well as J.-O. Persson from the Department of Mathematics at Stockholm University for his statistical advice.

SUPPLEMENTARY MATERIALS

www.sciencemag.org/content/350/6265/1248/suppl/DC1
Materials and Methods
Figs. S1 to S7
Tables S1 to S4
References (*33*–*62*)

28 July 2015; accepted 3 November 2015
10.1126/science.aad1010

NEURODEVELOPMENT

Single-cell transcriptomics reveals receptor transformations during olfactory neurogenesis

Naresh K. Hanchate,[1] Kunio Kondoh,[1] Zhonghua Lu,[1] Donghui Kuang,[1] Xiaolan Ye,[1] Xiaojie Qiu,[2,3] Lior Pachter,[4] Cole Trapnell,[2]* Linda B. Buck[1]*

The sense of smell allows chemicals to be perceived as diverse scents. We used single-neuron RNA sequencing to explore the developmental mechanisms that shape this ability as nasal olfactory neurons mature in mice. Most mature neurons expressed only one of the ~1000 odorant receptor genes (*Olfrs*) available, and at a high level. However, many immature neurons expressed low levels of multiple *Olfrs*. Coexpressed *Olfrs* localized to overlapping zones of the nasal epithelium, suggesting regional biases, but not to single genomic loci. A single immature neuron could express *Olfrs* from up to seven different chromosomes. The mature state in which expression of *Olfr* genes is restricted to one per neuron emerges over a developmental progression that appears to be independent of neuronal activity involving sensory transduction molecules.

Odor detection in mammals is mediated by odorant receptors on olfactory sensory neurons (OSNs) in the nasal olfactory epithelium (*1*, *2*). In mice, ~1000 odorant receptor genes (*Olfrs*) and 350 pseudogenes reside at dozens of distinct loci on 17 of 21 chromosomes (*3*–*5*). Each *Olfr* is expressed by a small subset of OSNs scattered in one epithelial spatial zone (*6*–*8*). Previous studies suggest that each mature OSN expresses one intact *Olfr* allele, but some coexpress an *Olfr* pseudogene (*9*–*11*). In a prevailing model of "OR [*Olfr*] gene choice," the developing OSN selects a single *Olfr* allele for expression, and the encoded receptor provides feedback that prevents expression of other *Olfrs* (*12*–*17*). OSNs are generated in a developmental progression from progenitors to precursors to immature OSNs to mature OSNs (*18*, *19*). We investigated when and how the developing OSN selects one *Olfr* for expression.

We used single-cell RNA sequencing (RNA-seq) (*20*) to analyze the transcriptomes of single epithelial neurons during development. We first prepared cDNA libraries from single isolated cells (*10*) and analyzed the libraries for markers of the four stages of OSN development, using polymerase chain reaction. We then conducted Illumina sequencing (*21*) of libraries from multiple cells in each stage, as well as duplicate libraries from some cells. We used TopHat (*22*) and Cufflinks (*23*) to identify genes expressed in each cell and to estimate their relative mRNA abundances (see fig. S1 for technical quality metrics).

We compared 85 cell transcriptomes using Monocle, an unsupervised algorithm that determines each cell's stage of differentiation in "pseudotime," which represents progress through gene expression changes during development (*24*). Monocle showed a linear nonbranching trajectory of development (Fig. 1A). Based on cell stage markers in individual transcriptomes, the trajectory reflects the developmental progression from progenitors through mature OSNs. The following gene markers were used: for progenitors, *Ascl1* (achaete-scute complex homolog 1); for precursors, *Neurog1* (neurogenin 1) and/or *Neurod1* (neurogenic differentiation 1); for immature OSNs, *Gap43* (growth-associated protein 43) and/or *Gng8* (guanine nucleotide–binding protein gamma 8); and for mature OSNs, *Omp* (olfactory marker protein) and four olfactory sensory transduction molecules downstream of odorant receptors—*Gnal* (guanine nucleotide binding protein, alpha stimulating, olfactory type), *Adcy3* (adenylate cyclase 3), *Cnga2* (cyclic nucleotide gated channel alpha 2), and *Cnga4* (cyclic nucleotide gated channel alpha 4) (*18*, *19*).

Immature OSNs were further divided into two subsets based on their expression of olfactory sensory transduction molecules. Early immature OSNs lacked one or more olfactory transduction molecules, whereas late immature OSNs expressed all four (Fig. 2).

A total of 3830 genes were differentially expressed over development. Clusters of genes changed in expression during specific developmental periods, suggesting sequential large and coordinated changes in gene expression during OSN development (Fig. 1B and table S1). By gene ontology, most clusters contained genes associated with transcriptional regulation and/or chromatin modification, suggesting potential regulators of development (table S1). In kinetic diagrams, markers of early and late

[1]Howard Hughes Medical Institute, Basic Sciences Division, Fred Hutchinson Cancer Research Center, 1100 Fairview Avenue North, Seattle, WA 98109, USA. [2]Department of Genome Sciences, University of Washington, Seattle, WA 98115, USA. [3]Molecular and Cellular Biology Program, University of Washington, Seattle, WA 98115, USA. [4]Departments of Mathematics, Molecular and Cell Biology, and Electrical Engineering and Computer Sciences, University of California–Berkeley, Berkeley, CA 94720, USA.
***Corresponding author. E-mail: coletrap@uw.edu (C.T.); lbuck@fhcrc.org (L.B.B.)**

developmental stages show peak expression early and late in the developmental progression, respectively (Fig. 1C and fig. S2).

Olfr expression first appeared at the late precursor to early immature OSN stages (Fig. 2). *Olfr* transcripts were found in one of nine precursors, 38 of 40 immature OSNs, and 25 of 25 mature OSNs (Fig. 2). None were seen in two non-neuronal epithelial supporting cells or in three cells of undetermined type. Overall, the number of *Olfr* transcripts per cell increased over OSN development (Fig. 2A). In early immature, late immature, and mature OSNs, *Olfrs* were detected at an average of 1998, 4146, and 8169 FPKM (fragments per kilobase of transcript per million mapped reads), respectively, with median values of 930, 2575, and 4026 FPKM. Transcripts of individual *Olfrs* were detected at an average of 657, 2156, and 6382 FPKM, with median values of 99, 807, and 2672 FPKM.

These studies indicate that the developing OSN can initially express multiple *Olfrs* (Fig. 2). Roughly half (48%, 12 of 25) of early immature OSNs with *Olfrs* expressed >1 *Olfr*. Coexpression of different *Olfrs* in single neurons declined as development progressed, with 46% (6 of 13) of late immature and 24% (6 of 25) of mature OSNs expressing >1 *Olfr*. Moreover, single early immature OSNs expressed up to 12 different Olfrs, whereas mature OSNs with >1 *Olfr* expressed two or at most three (Fig. 2B).

Early immature and mature OSNs with >1 *Olfr* also differed in the relative abundance of different *Olfr* transcripts (Fig. 2C). Most (10 of 12) of the early immature OSNs had similarly low levels of different *Olfrs*. The most abundant *Olfr* was detected at 55 to 396 FPKM in individual neurons and the next highest at, on average, 60.5% of this level (median, 60.1%). However, in three of six mature OSNs with >1 *Olfr*, the most abundant was detected at 14,557 to 18,056 FPKM, with the next highest, on average, only 3.3% as abundant (median, 0.5%).

In mature OSNs, *Olfr* and *Omp* transcripts averaged 8169 and 10,167 FPKM per cell, respectively. However, 6 of 12 early immature OSNs that expressed >1 *Olfr* did not express *Omp* (Fig. 2D), arguing against the possibility that the *Olfr* transcripts detected were due to contamination from mature OSNs.

Data from eight duplicate cell samples (technical replicates) were analyzed (figs. S3 and S4). The duplicates confirmed the expression of >1 *Olfr* in specific OSNs (table S2). The data were consistent with reported stochastic losses of low–copy number transcripts in single-cell RNA-seq data. *Olfrs* present in both replicates tended to be expressed at higher levels, and those present in only one replicate tended to be expressed at lower levels.

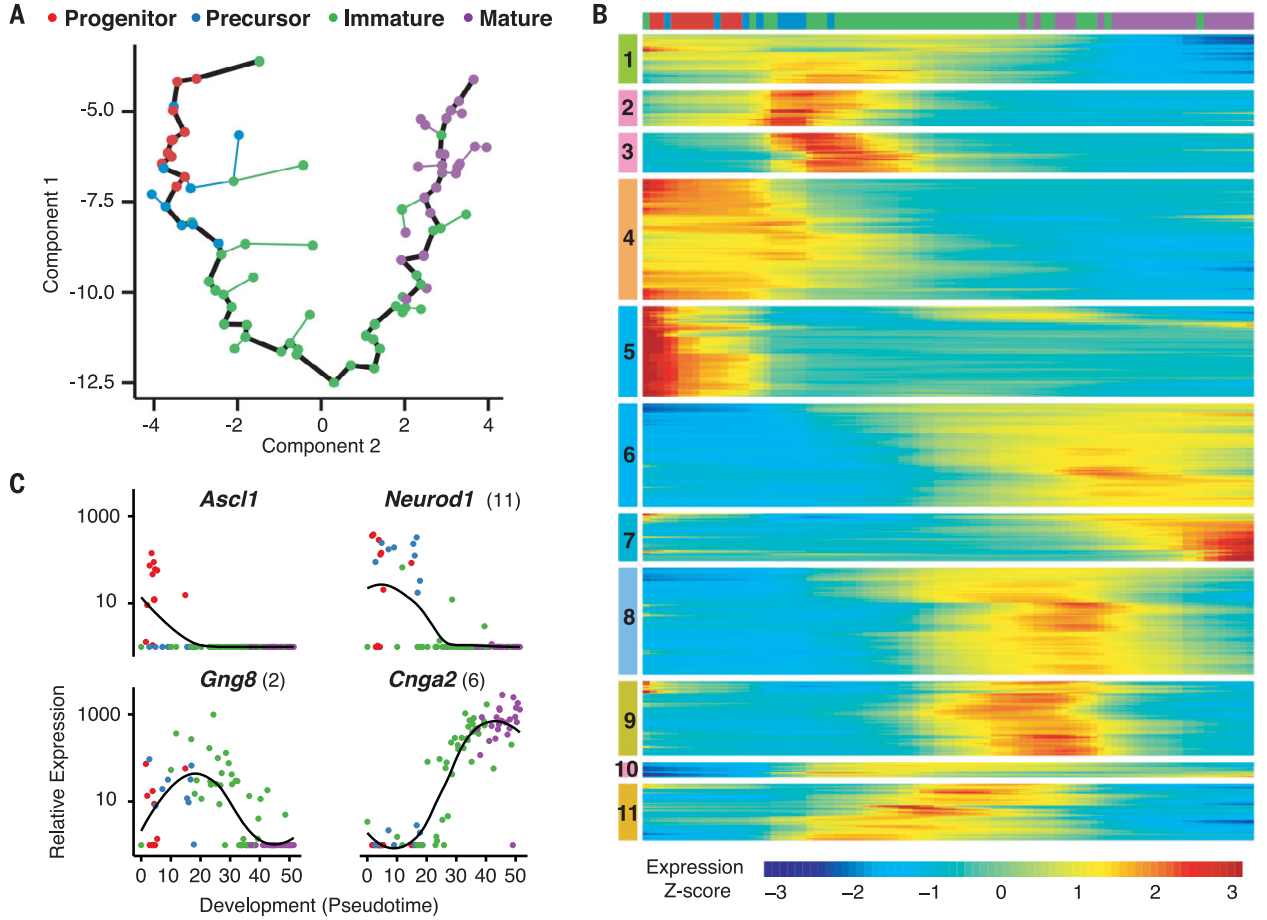

Fig. 1. Olfactory neurons exhibit large-scale shifts in gene expression during development. (**A**) Unsupervised analysis of single-cell gene expression profiles with Monocle revealed a linear trajectory (black line) along which cells develop in pseudotime. Coloring of cells based on the expression of developmental markers shows that the trajectory corresponds to a stepwise development from olfactory progenitors to precursors to immature OSNs to mature OSNs. (**B**) Global analysis of gene expression kinetics along the trajectory identified 3830 genes that vary significantly over developmental pseudotime (false discovery rate < 5%, determined by a Tobit-valued generalized linear model likelihood ratio test; supplementary materials). Hierarchical clustering of these genes via Ward's method recovered 11 nonredundant groups that covary over the trajectory. Cluster analysis indicates that multiple large shifts in gene expression occur as neurons progress through development. The bar on top shows the locations of individual cells, colored by stage of development, along this developmental trajectory. The Expression Z score indicates changes in a gene relative to its dynamic range over pseudotime. (**C**) Kinetic diagrams show the expression of known markers of different developmental stages over the developmental progression. Numbers in parentheses indicate the groups in which genes are found in (B). Dots indicate individual cells and are colored according to developmental stage. Black lines indicate local polynomial regression smoothing (span, 0.75; degree, 2) of log-transformed FPKM values over developmental pseudotime.

The above results indicate that early immature OSNs can express low levels of multiple *Olfrs*, but, during subsequent development, two changes typically occur. Expression favors one *Olfr* by up to 100 times or more, and the expression of additional *Olfrs* declines or disappears.

To validate these findings, we used RNA–dual fluorescence in situ hybridization (dual RNA-FISH) with nasal tissue sections. At postnatal day 3 (P3), a peak time of OSN neurogenesis (*19*, *25*), 0.22 ± 0.05 to 0.22 ± 0.12% of neurons labeled for a single *Olfr* were colabeled with a mix of probes for other *Olfrs* expressed in the same nasal zone (Fig. 3A and table S3). Neurogenesis decreases as mice mature, and no colabeled cells were seen in adults. Using a highly sensitive RNA-FISH method with branched DNA signal amplification (*26*), 0.41 ± 0.09 to 0.60 ± 0.13% of cells labeled for one *Olfr* were co-labeled for another *Olfr* at P3, and 0.10 ± 0.02 to 0.18 ± 0.05% were co-labeled for another at P21 (Fig. 3B and table S4). Among neurons labeled for one *Olfr*, the percentage co-labeled for the immature OSN markers *Gap43* and *Gng8* also changed, respectively, from 80.1 ± 3.2% and 62.8 ± 0.9% at P3 to 19.5 ± 0.5% and 14.3 ± 1.1% at P21 (table S5). These results confirm that single OSNs can express more than one *Olfr* and suggest that *Olfr* coexpression occurs predominantly, if not exclusively, in immature OSNs.

To examine whether odorant receptor–induced neuronal activity might be involved in the observed developmental shift in *Olfr* expression, we analyzed transcriptome data for the expression of olfactory sensory transduction molecules: *Gnal* (or *Gnas*, which may substitute for *Gnal*), *Adcy3*, *Cnga2*, and *Cnga4*. All four molecules were expressed in 6 of 18 immature OSNs and 6 of 6 mature OSNs with >1 *Olfr* (Fig. 2D). Furthermore, one or more were absent in data from 13 of 20 immature and 3 of 19 mature OSNs with only one *Olfr*. These results suggest that odorant receptor–induced neuronal activity is neither necessary nor sufficient for the decline in coexpressed *Olfrs* during development.

We next tested whether the developing OSN is restricted to activating *Olfrs* expressed in a particular nasal zone. Using dual RNA-FISH, we compared the nasal expression patterns of 11 pairs of *Olfrs* coexpressed in six different OSNs. In every case, the paired *Olfrs* were expressed either in the same spatial zone or in partially overlapping zones (Fig. 3C and table S6). These results suggest that the developing neuron is restricted to the expression of a particular *Olfr* regional gene set, which can include *Olfrs* with only partially overlapping expression patterns in the adult.

To investigate whether early coexpression of multiple *Olfrs* could result from chromatin changes at a single genomic locus containing those *Olfrs*, we determined the chromosome locations of *Olfrs* coexpressed in individual OSNs. For OSNs expressing 4 to 12 *Olfrs*, coexpressed *Olfrs* mapped

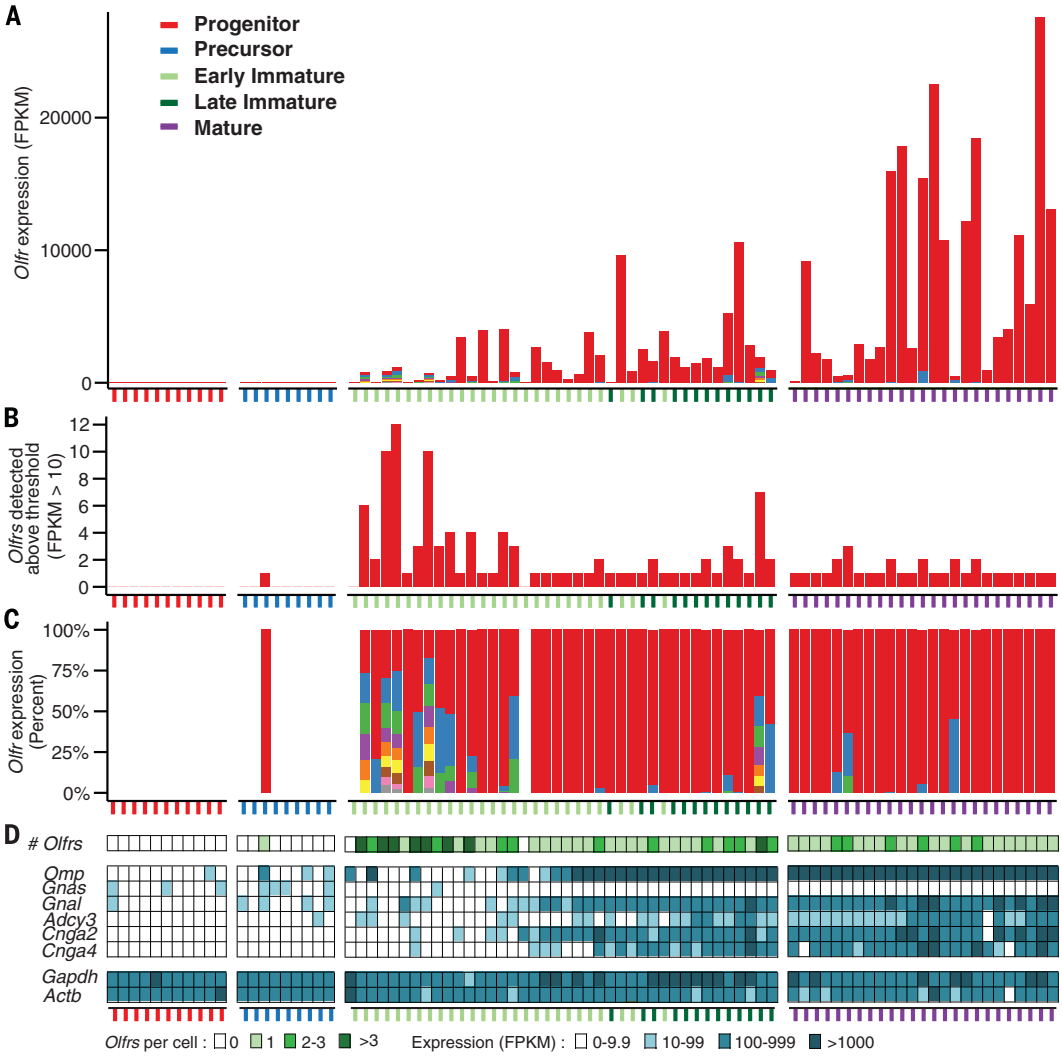

Fig. 2. Immature neurons can express multiple *Olfrs*. (**A**) Neurons assigned to different developmental stages were arranged by developmental progress, as measured in pseudotime. Different developmental stages are indicated by differently colored ticks. Different *Olfrs* are represented by different colors in the bars. The total number of *Olfr* transcripts per cell shows a steady, though variable, increase during development. (**B**) Multiple different *Olfr* transcripts were detected in 12 of 25 early immature, 6 of 13 late immature, and 6 of 25 mature OSNs with *Olfr* transcripts. (**C**) The number of different *Olfr* transcripts per cell was highest in early immature OSNs and then declined over development. Early immature OSNs tended to express similar levels of different *Olfrs*. In contrast, the majority of mature OSNs expressed only one *Olfr* or high levels of one *Olfr* and low levels of one or two additional *Olfrs*. Each color in a bar represents a single *Olfr*, except gray, which represents >1 *Olfr*. (**D**) *Olfrs* stimulate neuronal activity via mechanisms involving sensory transduction molecules encoded by *Gnal* (or possible *Gnas* in immature OSNs), *Adcy3*, *Cnga2*, and *Cnga4*. Six immature and six mature neurons with >1 *Olfr* expressed all four genes, suggesting that neuronal activity downstream of odorant receptors is not what reduces the number of *Olfrs* expressed per neuron. *Omp*, which is highly expressed in mature OSNs, was absent from six early immature OSNs with >1 *Olfr*, arguing against contamination from mature OSNs. *Gapdh* and *Actb* are housekeeping genes.

to three to seven different chromosomes and four to nine distinguishable *Olfr* gene loci (Fig. 4 and table S7). Thus, the immature OSN is not restricted to expressing *Olfrs* from a single chromosomal region.

Odor detection in the mouse nose is mediated by 1000 different odorant receptors, each expressed by a different subset of sensory neurons. We asked when and how a neuron comes to express a single *Olfr*. We found that the developing neuron can express low levels of multiple *Olfrs*. As development proceeds, this ability declines. The mature neuron typically expresses high levels of a single *Olfr*. Coexpressed *Olfrs* tend to be expressed by other neurons in the same region of the olfactory epithelium, suggesting regional biases in *Olfr* gene choice, but they can reside at multiple chromosomal locations.

How does the developing OSN transition from expressing low levels of multiple *Olfrs* to expressing a high level of a single *Olfr*? One possibility is a "winner-take-all" mechanism. In this model, multiple *Olfrs* are initially expressed, but one becomes dominant—for example, by the capture of limiting factors required for high-level *Olfr* expression (fig. S5). In an alternative model, selection of a single *Olfr* for high-level expression occurs independently of those initially expressed. In either model, early low-level expression of other *Olfrs* could subside, owing to the closing of a developmental time window or to feedback signals generated by the highly expressed *Olfr*. OSNs expressing multiple *Olfrs* are probably not pruned by apoptosis, as suggested for OSNs in the nasal septal organ (*27*), given genetic evidence that some OSNs expressing one *Olfr* previously expressed another (*13*). This *Olfr* "switching" may reflect the early expression of more than one *Olfr* per immature OSN, as observed in this study.

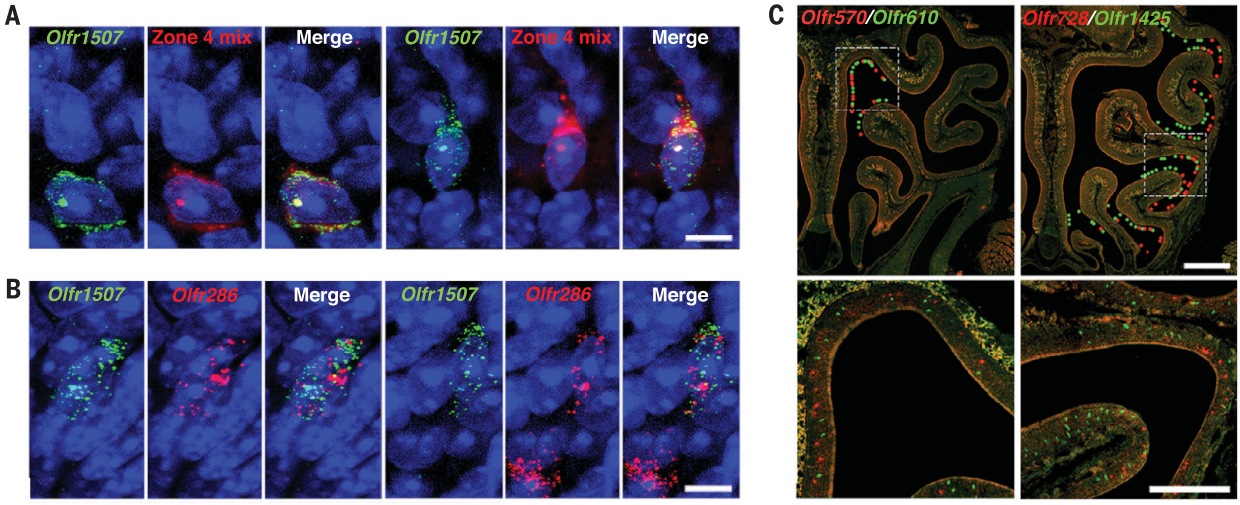

Fig. 3. *Olfrs* expressed in the same neuron belong to a regional gene set. (**A**) Dual RNA-FISH of P3 tissue sections using a conventional method showed a small percentage of OSNs co-labeled with an *Olfr1507* probe and a mix of probes for other *Olfrs* expressed in the same zone (zone 4). Cell nuclei were counterstained with 4',6-diamidino-2-phenylindole (blue). Two co-labeled cells are shown, one on the left half and the other on the right half of the panel. Scale bar, 5 μm. (**B**) Dual RNA-FISH of P3 tissue sections using a highly sensitive method showed a small percentage of OSNs coexpressing *Olfr1507* and *Olfr286*. Two co-labeled cells are shown [as in (A)], and a cell labeled with only one probe (red only) is also shown on the right. Scale bar, 5 μm. (**C**) Dual RNA-FISH shows that *Olfrs* coexpressed in single immature OSNs (neurons D200 or D243) are singly expressed in neurons in the same or partially overlapping zones in adult olfactory epithelium sections. This correspondence suggests that *Olfr* expression in the immature OSN is restricted to a spatially determined set of *Olfr* genes. In the upper row, colored dots indicate the locations of labeled neurons. Boxed areas in the upper row are shown at higher magnification in the lower row. Scale bars, 500 μm (upper row) and 250 μm (lower row).

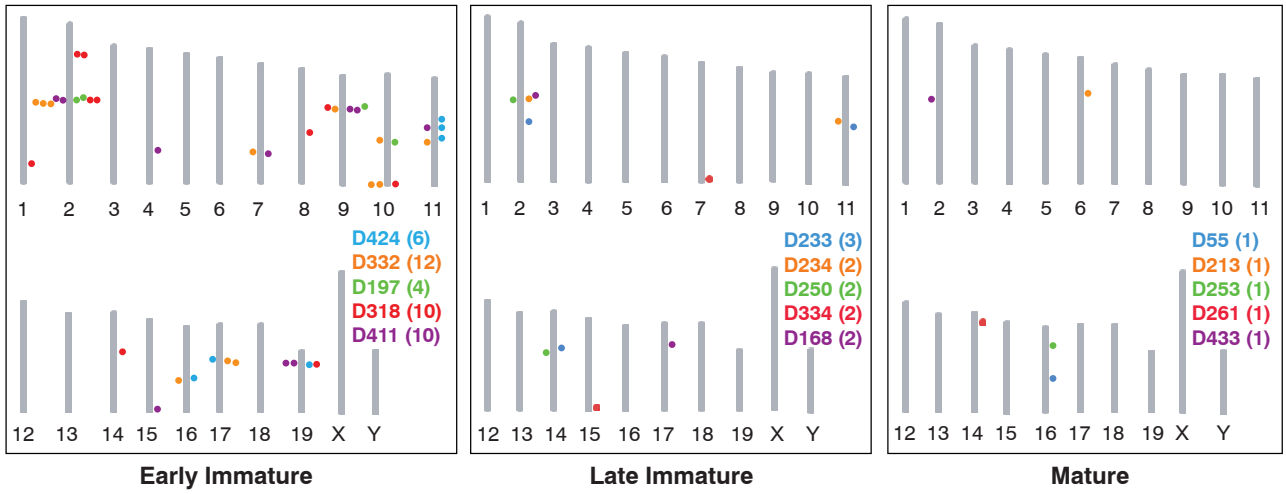

Fig. 4. Immature neurons coexpress *Olfrs* from multiple chromosomal loci. Diagrams show the chromosomal locations of *Olfrs* expressed in single OSNs of different stages. Each mouse chromosome is indicated by a vertical bar with its number below. The names of neurons, parenthesized number of *Olfrs* per neuron, and dots indicating the chromosomal locations of those *Olfrs* are shown in different colors for different neurons.

REFERENCES AND NOTES

1. L. Buck, R. Axel, *Cell* **65**, 175–187 (1991).
2. L. B. Buck, C. Bargmann, in *Principles of Neuroscience*, E. Kandel, J. Schwartz, T. Jessell, S. Siegelbaum, A. J. Hudspeth, Eds. (McGraw-Hill, New York, 2012), pp. 712–742.
3. X. Zhang, S. Firestein, *Nat. Neurosci.* **5**, 124–133 (2002).
4. P. A. Godfrey, B. Malnic, L. B. Buck, *Proc. Natl. Acad. Sci. U.S.A.* **101**, 2156–2161 (2004).
5. Y. Niimura, M. Nei, *Gene* **346**, 13–21 (2005).
6. K. J. Ressler, S. L. Sullivan, L. B. Buck, *Cell* **73**, 597–609 (1993).
7. R. Vassar, J. Ngai, R. Axel, *Cell* **74**, 309–318 (1993).
8. K. Miyamichi, S. Serizawa, H. M. Kimura, H. Sakano, *J. Neurosci.* **25**, 3586–3592 (2005).
9. A. Chess, I. Simon, H. Cedar, R. Axel, *Cell* **78**, 823–834 (1994).
10. B. Malnic, J. Hirono, T. Sato, L. B. Buck, *Cell* **96**, 713–723 (1999).
11. S. Serizawa *et al*., *Science* **302**, 2088–2094 (2003).
12. S. Serizawa, K. Miyamichi, H. Sakano, *Trends Genet.* **20**, 648–653 (2004).
13. B. M. Shykind *et al*., *Cell* **117**, 801–815 (2004).
14. J. W. Lewcock, R. R. Reed, *Proc. Natl. Acad. Sci. U.S.A.* **101**, 1069–1074 (2004).
15. R. P. Dalton, D. B. Lyons, S. Lomvardas, *Cell* **155**, 321–332 (2013).
16. M. Q. Nguyen, Z. Zhou, C. A. Marks, N. J. Ryba, L. Belluscio, *Cell* **131**, 1009–1017 (2007).
17. R. P. Dalton, S. Lomvardas, *Annu. Rev. Neurosci.* **38**, 331–349 (2015).
18. D. J. Nicolay, J. R. Doucette, A. J. Nazarali, *Cell. Mol. Neurobiol.* **26**, 801–819 (2006).
19. D. J. Rodriguez-Gil *et al*., *Proc. Natl. Acad. Sci. U.S.A.* **112**, 5821–5826 (2015).
20. S. Islam *et al*., *Genome Res.* **21**, 1160–1167 (2011).
21. D. R. Bentley *et al*., *Nature* **456**, 53–59 (2008).
22. D. Kim *et al*., *Genome Biol.* **14**, R36 (2013).
23. C. Trapnell *et al*., *Nat. Biotechnol.* **28**, 511–515 (2010).
24. C. Trapnell *et al*., *Nat. Biotechnol.* **32**, 381–386 (2014).
25. J. W. Hinds, P. L. Hinds, *J. Comp. Neurol.* **169**, 15–40 (1976).
26. M. L. Collins *et al*., *Nucleic Acids Res.* **25**, 2979–2984 (1997).
27. H. Tian, M. Ma, *Mol. Cell. Neurosci.* **38**, 484–488 (2008).

ACKNOWLEDGMENTS

We thank J. Delrow, A. Marty, and A. Dawson at the Fred Hutchinson Cancer Research Center (FHCRC) Genomics Facility for assistance with RNA-seq; M. Fitzgibbon and J. Davidson at the FHCRC Bioinformatics Resource for early assistance with sequence analyses; and J. Vasquez and the FHCRC Scientific Imaging Facility for help with confocal microscopy. We also thank members of the Buck laboratory for helpful discussions. This work was supported by the Howard Hughes Medical Institute (L.B.B.), NIH grants R01 DC009324 (L.B.B.) and DP2 HD088158 (C.T.), an Alfred P. Sloan Fellowship (C.T.), and a Dale F. Frey Award for Breakthrough Scientists from the Damon Runyon Cancer Research Foundation (C.T.). L.B.B. is on the Board of Directors of International Flavors & Fragrances. The supplementary materials contain additional data. N.K.H., C.T., and L.B.B. designed the research; N.K.H. and C.T. performed the research; N.K.H., C.T., K.K., Z.L., D.K., X.Y., X.Q., and L.B.B. analyzed the data; L.P. provided guidance; and N.K.H, C.T., and L.B.B. wrote the paper. Raw sequencing data related to this study have been archived in the Gene Expression Omnibus (GEO) database under accession number GSE75413 (available at www.ncbi.nlm.nih.gov/geo/query/acc.cgi?acc=GSE75413).

SUPPLEMENTARY MATERIALS

www.sciencemag.org/content/350/6265/1251/suppl/DC1
Materials and Methods
Figs. S1 to S5
Tables S1 to S7
References (*28*–*35*)

13 August 2015; accepted 27 October 2015
Published online 5 November 2015
10.1126/science.aad2456

PROTECTED AREAS

Protected areas and global conservation of migratory birds

Claire A. Runge,[1,2]* James E. M. Watson,[1,3] Stuart H. M. Butchart,[4] Jeffrey O. Hanson,[5] Hugh P. Possingham,[5,6] Richard A. Fuller[5]

Migratory species depend on a suite of interconnected sites. Threats to unprotected links in these chains of sites are driving rapid population declines of migrants around the world, yet the extent to which different parts of the annual cycle are protected remains unknown. We show that just 9% of 1451 migratory birds are adequately covered by protected areas across all stages of their annual cycle, in comparison with 45% of nonmigratory birds. This discrepancy is driven by protected area placement that does not cover the full annual cycle of migratory species, indicating that global efforts toward coordinated conservation planning for migrants are yet to bear fruit. Better-targeted investment and enhanced coordination among countries are needed to conserve migratory species throughout their migratory cycle.

From the writings of Aristotle (*1*) to the musings of Gilbert White in Georgian England (*2*), migratory birds have fascinated and inspired people for generations. Migrants undertake remarkable journeys, from endurance flights exceeding 10,000 km by bar-tailed godwits (*Limosa lapponica*) (*3*) to the annual relay of arctic terns (*Sterna paradisaea*), which fly the equivalent of the distance to the moon and back three times during their lives (*4*). Migratory species make major contributions to resource fluxes, biomass transfer, nutrient transport, predator-prey interactions, and food-web structure within and among ecosystems (*5*) and play an important role in human culture (*6*). Yet more than half of migratory birds across all major flyways have declined over the past 30 years (*7*).

Threats in any one part of a annual cycle can affect the entire population of a migratory species (*8*), and so environmental management actions for migrants need to be coordinated across habitat types, seasons, and jurisdictions (*8*). Protected area designation is a widely used approach for averting species loss (*9*) because it can reduce habitat loss, habitat degradation, hunting pressure, and disturbance (*10*). Yet the extent to which the distributions of migratory species are covered by protected areas globally is poorly understood. Many previous global and regional species conservation assessments and prioritization analyses either omit parts of the annual cycle or treat all species' distributions as static (*9*–*12*). Here, we explore how protected area coverage of migratory birds varies across their annual cycle and among countries and compare their current levels of protected area coverage against standard conservation targets. Overlaying maps of protected areas (*13*) onto distribution maps of the world's birds, we assessed whether the proportion of each species' distribution covered by protected areas met a target threshold (*9*, *11*). For migratory species, we set targets for each stage of the annual cycle separately for the 1451 migratory birds, with mapped distributions throughout their annual cycle.

We discovered that 91% of migratory bird species have inadequate protected area coverage for at least one part of their annual cycle, despite individual elements of the annual cycle being well protected for some species (Table 1). This is in stark contrast to 55% of nonmigratory species with inadequate protected area coverage across their global distribution. A typical migrant relies on two or three disjoint geographic locations, and the chance that they are all adequately conserved is probabilistically lower than for a single location (supplementary materials). We found that migratory species are less likely to meet protection targets as the number of seasonal areas increases and that the proportion of migratory species meeting targets is consistent with randomly allocated conservation effort (Fig. 1), indicating that despite widespread recognition of the need for an internationally coordinated approach to conservation of migratory species, protection is not yet systematically coordinated across the seasonal ranges of species. Twenty-eight migratory bird species have no coverage in at least one part of their annual cycle, and 18 of these have no protected area coverage of their breeding range. Two species lack any protected area coverage across their entire distribution (Table 1). Disturbingly, less than 3% of threatened migratory bird species have adequate protected area coverage across all parts of their annual cycle (table S1).

Widespread migrants may benefit more from broader-scale policy responses (such as targeting

[1]School of Geography, Planning and Environmental Management, University of Queensland, Brisbane, QLD, 4072, Australia. [2]National Center for Ecological Analysis and Synthesis (NCEAS), University of California, Santa Barbara, Santa Barbara, CA 93101, USA. [3]Global Conservation Program, Wildlife Conservation Society, New York, NY, USA. [4]BirdLife International, Wellbrook Court, Cambridge CB3 ONA, UK. [5]School of Biological Sciences, University of Queensland, Brisbane, QLD 4072, Australia. [6]Department of Life Sciences, Imperial College London, Silwood Park, Ascot, Berkshire SL5 7PY, England, UK.
***Corresponding author. E-mail: claire.runge@uqconnect.edu.au**

Single-cell transcriptomics reveals receptor transformations during olfactory neurogenesis

Naresh K. Hanchate, Kunio Kondoh, Zhonghua Lu, Donghui Kuang, Xiaolan Ye, Xiaojie Qiu, Lior Pachter, Cole Trapnell, and Linda B. Buck

Science **350** (6265), . DOI: 10.1126/science.aad2456

Maturation of olfactory neurons

The sense of smell depends on neurons in the olfactory epithelium to perceive chemical scents. Each neuron specializes with one receptor. Hanchate *et al.* now show that the one-for-one relationship is not as simple as thought. As new neurons develop to replenish the olfactory epithelium, they initially express several different alleles of olfactory receptors. Then, as each neuron matures, they specialize to express a single receptor.

Science, this issue p. 1251